New methodology to measure the dynamics of ocular wave front aberrations during small amplitude changes of accommodation

L. Diaz-Santana, V. Guériaux, G. Arden, and S. Gruppetta

Applied Vision Research Centre, Henry Wellcome Laboratories for Visual Science, Department of Optometry and Visual Science, City University, Northampton Square, London EC1V 0HB, UK

Abstract: We present a methodology to measure the systematic changes of aberrations induced by small changes in amplitude of accommodation. We use a method similar the one used in electrophysiology, where a periodic stimulus is presented to the eye and many periods (epochs) of the stimulus are averaged. Using this technique we have measured changes in higher order aberrations from 0.006 m to 0.02 m and correlated them with amplitude changes of accommodation as small as 0.14D. These small changes would have been undetectable without epoch averaging. The correlation coefficients of Zernike terms with defocus were calculated, demonstrating higher values of correlation for epoch averaging. The accurate monitoring of defocus at the start of the accommodation response has shown some interesting trends that may be related with the mechanisms behind accommodation.

OCIS codes: (010.7350) Wave-front sensing; (330.4460) Ophthalmic optics; (330.5370) Physiological optics

References and links

1. T. Young. "On the mechanism of the eye," Phil. Trans. **91**, 69 (1801).
2. J. Liang, B. Grimm, S. Goelz, and J.F. Bille. "Objective measurement of wave aberration of the human eye with the use of a Hartmann-Shack wave-front sensor," J. Opt. Soc. Am. A. **11**, 1949–1957 (1994).
3. H. Hofer, P.Artal, B.Singer, J.L Aragón, and D.R. Williams. "Dynamics of the eye's wave aberration," J. Opt. Soc. Am. A. **18**, 597–506 (2001).
4. H.T. Kasprzak and J. W. Jaronski. "Measurement of fine dynamic changes of the corneal topography by use of interferometry," In W. Osten, editor, Interferometer XI: Applications, SPIE–The International Society for Optical Engineering **4778**, 169–176 (2002).
5. L. Diaz-Santana, C. Torti, I. Munro, P. Gasson, and C. Dainty. "Benefit of higher closed–loop bandwidths in ocular adaptive optics," Opt. Express **11**, 2597–2605 (2003).
6. T. Nirmaier, G. Pudasaini, and J. Bille. "Very fast wavefront measurements at the human eye with a custom CMOS-based Hartmann–Shack sensor," Opt. Express **11**, 2704—2716 (2003).
7. D.R. Iskander, M.J. Collins, M.R. Morelande and M. Zhu. "Analyzing the dynamic wavefront aberrations in the human eye," IEEE Trans. Biomed. Eng. **51**, 1969–1980 (2004).
8. K. M. Hampson, I. Munro, C. Paterson, and C. Daint. "Weak correlation between the aberration dynamics of the human eye and the cardiopulmonary system," J. Opt. Soc. Am. A. **22**, 1241–1250 (2005).
9. J.J. Gicquel, J.L. Nguyen-Khoa, N. Lopez-Gil, R. Legras, P. Dighiero, D.A. Lebuisson, and J.F. Le Gargasson. "Optical aberrations variations of the human eye during accommodation," Invest. Ophthalmol. Vis. Sci. E-Abstract 1993:B762 (2005).
10. H. Cheng, J.K. Barnett, A.S. Vilupuru, J.D. Marsack, S. Kasthurirangan, R. A. Applegate, and A. Roorda. "A population study on changes in wave aberrations with accommodation," J. of Vision **4**, 272–280 (2004).

11. N. Davies, L. Diaz-Santana, and D. Lara-Saucedo. "Repeatability of ocular wavefront measurement," Optom. Vis. Sci. **80**, 142–150 (2003).
12. H. Ginis, S. Plainis, and A. Pallikaris. "Variability of wavefront aberration measurements in small pupil sizes using a clinical shack-hartmann aberrometer," BMC Ophthalmology **4**, 1471–2415 (2004).
13. R.B Rabbetts. Bennett & Rabbetts Clinical Visual Optics. Butterworth and Heinemann, 5th edition (1998).
14. A. Dubinin, T. Cherezova, A. Belyakov and A. Kudryashov. Human eye anisoplanatism: eye as a lamellar structure. In F. Manns, P. G. Söderberg, and A. Ho, editors, Ophthalmic Technologies XVI. Edited by Manns, Fabrice; Söderberg, Per G.; Ho, Arthur. Proceedings of the SPIE, **6138**, 260–266 (2006).
15. J. Arines. *Imagen de alta resolución del fondo de ojo por deconvolución tras compensacion parcial*. PhD thesis, Universidade de Santiago de Compostela (2006).
16. ANSI. *American national standard for ophtalmics. ANSI-Z80.28-2004, Methods for reporting optical aberrations of eyes*. American national standards institute, Inc. (2004).
17. L. Diaz Santana Haro and J.C. Dainty. "Effects of retinal scattering in the ocular double–pass process," J. Opt. Soc. Am. **18**, 1437–1444 (2001).
18. L. Diaz Santana Haro and J.C. Dainty. "Single–pass measurements of the wave-front aberrations of the human eye by use of retinal lipofuscin autofluorescence," Opt. Lett. **24**, 61–63 (1999).
19. H. Li and C. Rao. "Precision analysis of hartmann-shack wave-front sensor with modal reconstruction," J. Phys. Conference Series **48**, 952–956 (2006).
20. J.S. Wolffsohn, B. Gilmartin, E.A. Mallen, and S. Tsujimura. "Continuous recording of accommodation and pupil size using the shin-nippon srw-5000 autorefractor," Ophthalmic Physiol. Opt. **21**,108–113 (2001).
21. David Regan. *Human Brain Electrophysiology. Evoked Potentials and Evoked Magnetic Fields in Science and Medicine*. Elsevier Science Publishing, (1989).

1. Introduction

The human eye is a dynamic system: ocular movements, saccades, blinking, changes in accommodation and pupil size and configuration of the tear film, amongst other physiological changes are a continuous response of the eye to maintain a clear retinal image. It has been known for more than two centuries that aberrations affect the optical quality of the eye [1]. In 1994 Liang and Bille [2] proposed to use a Shack-Hartmann (SH) sensor to measure these aberrations.

A SH uses an array of micro-lenses to split the light reflected from the retina in a regular pattern of spots. An aberration free eye would produce a perfectly regular pattern of spots. Such an image is usually referred as a *reference frame* and the beam producing it as a *reference beam*. An aberrated eye instead produces an irregular pattern of spots. The distance each spot moves away from its perfect position in the reference frame is proportional to the gradient of the wavefront at the corresponding pupil position. Image processing enables to measure these displacements and obtain a gradient map of the wavefront, from where it is possible to reconstruct the ocular wavefront. Typically a least square fit to a Zernike polynomial expansion is used to reconstruct it. Its implementation has been described in detail elsewhere [2]. This methodology has been used extensively to measure static aberrations. However, the dynamics of these aberrations beyond defocus and astigmatism have not been as extensively studied [3, 4, 5, 6, 7, 8].

Hofer *et al*. [3] studied the dynamics of eye aberrations using SH images at a frame rate of 65 images/s. In their analysis they studied the changes over time of the wavefront root mean square (RMS) error, as this quantity is a well established metric of optical performance. They calculated the power spectrum of these temporal series and found that it presented a very characteristic behaviour for all eyes studied: when plotted in log-log scale it appeared as a straight line with a negative slope of -1.5, up to 12Hz. A later study by Diaz-Santana *et al*. observed similar behavior down to 30Hz [5], while another work by Nirmaier *et al*. found similar behavior down to 70Hz [6]. The mechanisms behind this behaviour have not yet been understood.

One important aspect of aberration dynamics is their relationship with accommodation. Recently Gicquel *et al*. [9] measured dynamic changes of accommodation by recording aberrations for 6 different decreasing accommodative stimuli varying from 5D to 1D with 0.5D steps in 14 subjects. Each measurement was repeated 3 times. They found an increment in wavefront

RMS with accommodation. Cheng *et al*. [10] studied a large population. They measured ocular aberrations at infinity, 3D and 6D of accommodation. They collected at least 3 aberration measurements for each accommodative step. They found that changes in the wavefront RMS are due mainly to the contribution of spherical aberration and 3rd order coma during accommodation.

In general, the measured variability of ocular aberrations both in a relaxed eye and during accommodation, is a combination of system noise and actual aberration variability. It has been shown in the past that variability of aberrations must be taken into account when doing aberration measurements. Davies *et al*. [11] showed that misalignment of the subject with respect to the system is a source of error and averaging must be done to reduce this problem. Ginis *et al*. [12] studied the dynamics of aberrations using 50 measurements from four eyes. They found that the signal to noise ratio (S/N ratio) was lower for higher order aberrations than for lower ones, and that a number of Zernike coefficients were below the noise level. They concluded that wavefront aberration data should be extracted from an average measurement as the aberrations are a dynamic quantity.

The dynamic changes departing from the mean value of ocular aberrations recorded over time have the following properties: (a) changes in the signal are often below the noise level, (b) the amplitude of this variability can be dependent on any stimulus presented to the subject, and (c) this signal can be regarded as either a steady state or a transient signal. These properties are the same as found in brain electrophysiology measurements, which prompts us to apply signal analysis techniques developed for electrophysiology to aberration dynamics.

Electrophysiology has over the years developed a large, robust and well tested battery of methods used to extract and analyse valid signals from noisy backgrounds. These methods are largely dependant on well designed experiments matched by equally robust data analysis techniques. One such standard technique is that of collecting repeated averages. In it, a temporally periodic stimulus is presented to the subject. Each period is called an *epoch*, and an average of a large number of epochs is collected. This method assumes that the system (the brain) has the same response to each stimulus (*stationarity*). Also, there is (implicitly) the assumption that the duration of the response is not longer than the averaging epoch. The full benefit of this method occurs when the amplitude of the response is of the same order of magnitude as the noise.

In the case of the eye, if we present a temporally periodic stimulus that induces accommodation changes, and it is true that the accommodation response will be constant to a particular stimulus, then we can use this technique to study the very small changes in aberrations that are induced by accommodation alone.

In this paper we validate this methodology inducing small changes of accommodation taking advantage of chromatic aberration of the eye. By reversing a checkerboard pattern between red and blue every two seconds we induce a change in vergence of about 1D. Due to physiological reasons [13], the accommodation response measured is smaller than this nominal value. This way, it is possible to run the experiment from a standard colour monitor without the need of building a motorised telescope. Results obtained from 4 subjects are presented in Section 3, showing how low amplitude aberrations that are driven at the same frequency as the stimulus are detectable with this methodology, but would otherwise be masked by noise.

2. Methodology

2.1. Optical Set-up

A SH wavefront sensor [2] that permits binocular viewing of a visual stimulus while recording wavefront aberration data at 24Hz from one eye was designed and implemented. A schematic of the set-up is shown in Fig. 1. A laser diode (LD) at 780nm is used as a light source. The beam is spatially filtered using a microscope objective (MO) and a pinhole (PH). Lens L1 collimates

the beam. An iris (I) is used to select the diameter of the beam sent into the eye. The beam has a maximum power of 10 W, which is safe to look into for more than 8 hours. A reference beam is obtained by fully opening the iris (I) and placing the removable mirror M4 as indicated.

For data collection the beam diameter is reduced to 1mm and the power on the eye becomes less than 1 W. This is so that the beam reaching the retina is diffraction limited, ensuring a high S/N ratio of the SH spots. At this stage mirror M4 is blocked so that only light from the retina reaches the SH sensor. The light back-scattered from the retina is used for wavefront sensing with a SH lenslet array coupled to a JAI CCD camera model CV-M50 IR. The eye pupil is conjugated with the SH lenslet array plane with the telescope formed with lenses L2 (f=250mm) and L3 (f=200mm). The focal length of L1 is set by the distance between the eye and the beamsplitter BM. At this magnification each lenslet subtends 750 m over the pupil plane. The lenslet array has a focal length of 40mm.

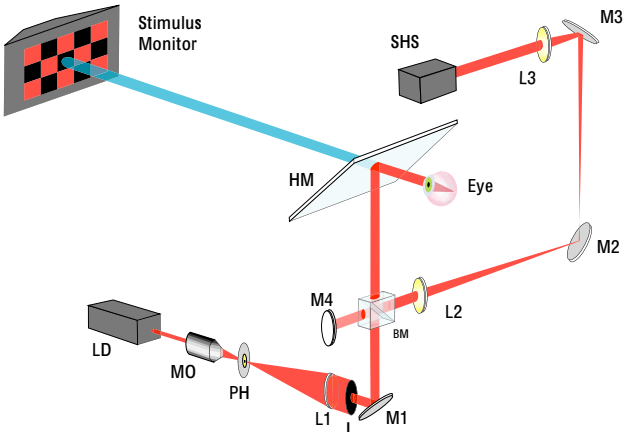

Fig. 1. Schematic representation of the Optical Set-Up

HM is a hot mirror (reflects infrared and transmits visible) 200mm×130mm that serves the double purpose of sending the IR light back-scattered from the eye into the wavefront sensing branch of the system whilst permitting visible light from the stimulus to be seen binocularly by the subject. Video images from the SH sensor are relayed to a Canon Digital Video Recorder MV700i where they are stored in Digital DV tape for later analysis. The system is mounted on a Keeler chinrest mount with a joystick similar to those in a table used in biomicroscopy of the anterior part of the eye in ophthalmic examinations. The subjects head is stabilised using the chinrest and the system is aligned with the subject's eye using the platform's joystick.

2.2. Stimuli

The window formed by the hot mirror between the sensor and the stimulus, together with the joystick alignment system, allows one to use the system with diverse visual stimuli. This can be from a target behind a variable focus system (like a variable power telescope or a badal system) for accommodation studies or a computer monitor. With this system it is possible to measure the dynamics of eye aberrations while performing several different visual tasks like reading, psychophysical experiments, or as in the case of our study, during accommodation.

For this experiment we used longitudinal chromatic aberration (LCA) in the eye to induce a change in focus. When red light (from the monitor) is focussed optimally on the retina, the focus of the blue squares will be in front of the retina. Hence by alternating blue and red images on the screen monitor it is possible to produce a small amplitude change of accommodation, as

the subject will try to keep the image in focus. Because the subjects were optimally corrected for far vision, placing the monitor at a distance of 60cm from the observer, implied that the blue stimulus was in focus, as the vergence from the distance of 60 cm was approximately equal in magnitude with the LCA of the eye between the edges of its spectral sensitivity. Presentation of the red stimulus then elicited an accommodation response as the near target would not be automatically in focus due to the opposite LCA for the red phosphor.

A red/black checkerboard was changed within one field time into a blue/ black checkerboard, and vice-versa. A change occurred every 2 seconds so a full cycle occupied 4s. (0.25Hz). The stimuli were presented on a MultiSync FE1250+, frame rate 75Hz monitor 60cm away from the eye. Each square check subtended 3.8deg of visual field and the full monitor subtended 33deg$\times$26deg. Luminance was measured to be constant. Subjects LD and SG did the experiments with a luminance of 1.2cd.m^{-2}, and subjects JZ and BT did the experiments at 0.2cd.m^{-2}. The change to a lower luminance was solely based on the fact that the pupil was larger and we could have more data points for wavefront sensing. As the spatial frequency of this stimulus is very low, we relayed on the harmonics of the checkerboard to elicit an accommodative response. That is, the response was prompted by the blurring of the checks' edges.

2.3. Data collection

The subject's head was stabilised on the chin rest and the dominant eye aligned with the system using the joystick platform. Alignment was achieved by placing the image with the SH spots in the centre of a monitor relaying the image obtained with the CCD. The iris was closed to its minimum aperture (about 1mm).

A few seconds of the stimulus were then presented to the subject if he was not familiar with the experiment. The subject was asked to fixate on the corner of the square check that appeared nearest to the red spot produced by the LD. This meant that there was always an off-set between the corner used for fixation and the sensing beam of less than 1.9 degrees. The isoplanatic patch of the eye has been estimated to be between 1.5 to 2.5deg [14], hence this off-set should be of little impact on the aberration measurements when compared against those ones measured foveally. However, if the differences were larger they would not affect the methodology presented as the off-set was kept constant throughout the data collection session. Once the subject was familiar with the experiment, he was realigned with the system, the stimulus was started again and data collection started within the next 30 seconds. Data was collected for 300 seconds.

In order to synchronise data from the eye the signal driving the monitor was split in two. One of the split signals was sent to drive the monitor, while the blue channel of the second split was sent to a National Instruments DAQ card. This same card was used to switch the input laser to the eye on and off in order to get a reference timing point in the video signal. We started collecting data from the signal used to drive the monitor at the same time as the laser was switched on. By starting video recording with the laser still off, we ensured that the first frame in the video with SH spots from the eye was synchronised with the signal driving the stimulus in the monitor to within 12ms. Data from the signal driving the monitor was collected at 240Hz, then averaged off-line to 24Hz, and binarised such that while the monitor was showing blue the recorded signal was one and zero while the red checks were displayed.

Data from the dominant eye of four subjects were collected. All subjects were male adults between 27 and 34 years old. None of them presented any known ocular pathology. Their prescriptions for their dominant eye were as follows: SG, LE, -3.0/-5.0$\times$169; LD, LE, +0.25/-0.50$\times$175; JZ, LE, -6.25D/-1.25$\times$50, BT, RE, -3.0/-0.25$\times$90. All subjects except LD wore their prescriptions while performing the experiment. SG wore contact lenses.

All sessions were run with all room lights switched off and only the stimulus and laser diode

beam reaching the eye. Two data sets were collected from subjects LD, SG and JZ, whilst only one data set was collected from subject BT. Data was collected for five minutes per set. The data set with the best S/N ratio in the SH images was analysed.

Either prior to the arrival of the subject or after data collection a reference beam was sent into the CCD camera and one second of data (24 images) recorded. The reference beam was recorded with the iris fully open, mirror M4 unblocked and the subject away from the system. The need for, and the use of the reference beam is described in detail in the section below.

2.4. Wavefront Reconstruction

The data from the DV tape was converted to individual *tiff* files using *iMovie*^{TM} software for MacOS 10.4. The files were saved with no compression at 24 frames per second. Custom-made wave front reconstruction software written in matlab^{TM} was used to analyse the individual files.

The software automatically finds the position of the reference beam spots from an average of 24 frames. The resulting matrix has the co-ordinates of all the spots that can form an image on the CCD. In contrast, the SH spots from an eye are constrained to be within an quasi-circular area defined by the eye pupil and smaller than the CCD. At each individual frame, the code decides if at each particular spot position defined by the reference the eye is forming a spot. For this, a low contrast is treated as no spot present, while a higher contrast is treated as a spot in that region. In this way it is possible to continuously track the SH spots positions as the eye moves around. Tracking the eye pupil using the centroids positions has been experimentally verified and has an accuracy as good as 50 m [15]. The program generates a reconstruction matrix for the particular group of lenslets used in each frame.

Additional inputs required are the pupil size over which to reconstruct the wavefront and the size of the area over which the centroiding of each spot is performed. Pupil size is kept fixed throughout all the analysis and only spots within that region are analysed. As accommodation induces a reduction in pupil size the smallest pupil recorded was chosen for analysis or the minimum size required to include 20 SH spots, whatever was larger.

Wavefront reconstrucion was done to 5th order, using a Zernike polynomial expansion (ANSI standard [16]). For this, a minimum of 20 spots was required, hence if less than this number was recorded, all Zernike coefficients were set to zero for that frame. This could occur during blinking, if the pupil size reduced beyond the value given for analysis, or sometimes some spots reduced their contrast below the threshold chosen due to speckle [17, 18]. Despite of these measures, the reconstruction occasionally failed due to other reasons; for example the fact that edge spots sometimes fail to fully fill the corresponding lenslet array creating a skewed image, and hence a large error close to the pupil boundary [19]. These anomalous frames appear as high peaks and are easily detected and automatically be removed by setting the values of all Zernike coefficients at those points to the mean value of the 15 frames before and 15 frames after them.

Once the pupil size and threshold values were fine tuned for each data set, the code could be left to run automatically. Analysis of such large data sets would have been impossible if larger user inputs were needed. By using C++ we expect in the future to be able to do this analysis in real time or close to real time while the data is being collected.

2.5. Epoch analysis and running averages

We assume that the aberrations of the eye respond with a periodic component with the same period as that of the stimulus. The analysis technique used, takes advantage of this periodic response and averages it over many periods. Additionally, we also expect a semi-random component that is a combination of other elements. Some of them are random, like the aberrations induced by the tear film, or the result of noise in the images like the speckle in the SH spots

or electronic noise. Some of these elements are periodic or quasi-periodic but with a different frequency than that of the stimulus, like those correlated with the cardiopulmonary system [8, 7]. With our methodology, any random aberration changes or periodic changes at different frequencies than the stimulus (or its harmonics) are averaged out of the signal.

Analysis was performed as follows: the reconstruction of the ocular wavefronts described in section 2.4, generates a matrix (7200×20) where each row is a vector (7200×1) containing the time series of a particular Zernike coefficient (from 1 to 20) at 24Hz. Each epoch lasts 4s or $4 \times 24 = 96$ data points. In order to average the signal by epochs, each row from this matrix is reshaped into a matrix (96×75), where now each row (96×1) is the realisation of one full stimulus cycle. If we consider each one of these rows as the full cycle of a periodic function, then all data points in each column correspond to the same phase of this periodic function. Averaging each one of these 1×75 column-vectors we obtain the *running average* over 4 seconds. Only if the eye response to the stimulus is a constant functional form of the same frequency, then this running average will give us access to that function. The output from this analysis is a matrix (96×20) where each row is the running average of 75 epochs of an individual Zernike coefficient over 4s.

We studied the variation in the S/N ratio as a function of the number of averages performed. For this, we modified the algorithm described above so that it was possible to change the number of epochs averaged, from one to all 75 collected. For each case the S/N ratio of each Zernike coefficient over the resultant running average was estimated. We then proceeded to calculate the variation of the correlation coefficient between defocus and each Zernike term, also as a function of the number of epochs averaged.

The S/N ratio is defined as the mean value of a signal divided by its standard deviation, and is usually expressed in decibels (dB). When estimating the SNR of the averaged epochs we only took the section of the signal that corresponded to the response to red. This was done to eliminate the step in the signal that represents the accommodation response. Similar results were obtained for the blue response.

We also estimated the correlation coefficients between defocus and the angle and amplitude of *Zernike pairs*. This approach has the advantage of being able to split (in some cases) rotations in the optical element from amplitude changes of aberrations. This may be important when studying changes in aberrations during accommodation and the role of torsion in these changes. We will come back to this in section 4.

The common way to represent Zernike terms in the literature is using the double index notation adopted by the ANSI standard [16]. In this notation Zernike coefficients are denoted by $C_m^{\pm n}$, where n is the meridional index, and n is the radial index. We call *Zernike pairs* all the non-rotationally symmetric terms with the same radial order and meridional indexes with the same magnitude. These pairs can be regarded as the two components of a vector in an angular space [16]. The magnitude and angle are given by Eqs. 1 and 2 respectively:

$$a_{nm} = \sqrt{\left(c_n^{-m}\right)^2 + \left(c_n^m\right)^2} \tag{1}$$

$$\theta_{nm} = \frac{\arctan\left(\frac{c_n^{-m}}{c_n^m}\right)}{|m|} \tag{2}$$

Figure 2 shows the interferograms of the resultant Zernikes terms after being paired with Eqs. 1 and 2. As the values of $C_m^{\pm n}$ in each pair change, the amplitude and orientation of the interferogram will change. The colours used below each image will be used to represent each pair later in section 3.

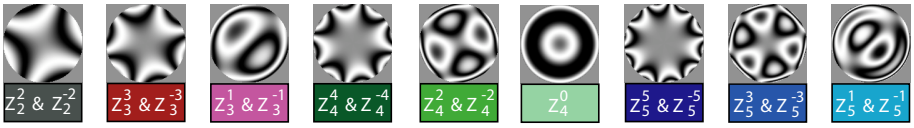

Fig. 2. Interferograms depicting the resultant zernike pairs using Eqs. 1 and 2. As the values of the Zernike coefficeints $C_m^{\pm n}$ in each pair change the amplitude and angle of the interferogram will vary. The colour code under each image will be used below in section 3. Z_4^0 has been included for completeness.

3. Results

3.1. Response of accommodation and signal improvement of low order aberrations

The stimulus presented produced a periodic change in accommodation as expected. In Fig. 3 we show the behaviour of the Zernike term for defocus C_2^0 as a function of time. The coloured regions behind the graph represent the colour of the stimulus during the corresponding time in the x-axis. In Fig. 3(a) we show a typical 12 seconds interval. This time series begins in the instant when the stimulus has just changed to red. In Fig. 3(b) we show the results of running averages. The time series begins one second after the change to red. The black line shows one single epoch with no averaging, the green line shows an average of 10 epochs, the blue line shows 30 epochs and the red one 75 epochs.

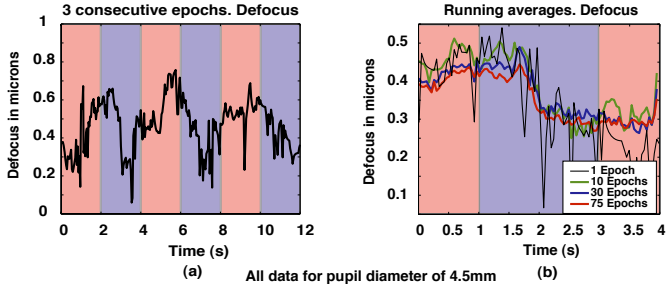

Fig. 3. Response of accommodation to the blue red stimuli. In both figures the areas in red correspond to the time when the stimulus was in red, and similarly for blue. (a) Measured changes in defocus over 12 seconds without any averaging. (b) Effect of running averages in the measurement of defocus. In black no averaging, green running average of 10 epochs, in blue 30 epochs and in red 75 epochs

Improvement in the S/N ratio is evident for all subjects in all 2^{nd} order aberrations (defocus and astigmatism). In Fig. 4 we show the changes in S/N ratio in dB for defocus and astigmatism as a function of the number of epochs averaged for all four subjects. Improvement in the S/N ratio permits clear visualisation of the accommodation response for all subjects. It allows accurate measurement of very small changes in accommodation and timing of the response. In Fig. 5 we show the accommodation response averaged over 75 epochs for each subject. We observe in all cases a delay of approximately 0.6sec between change of colour stimulus and start of the accommodative response. Subject LD was the most familiar with the stimulus, and correspondingly his accommodation response seemed the most precise. Note the trend to over-accommodate for the blue stimulus in all other subjects, and absent in LD.

It is clear that all four subjects focused at a different point (relative to the off-set of the SH

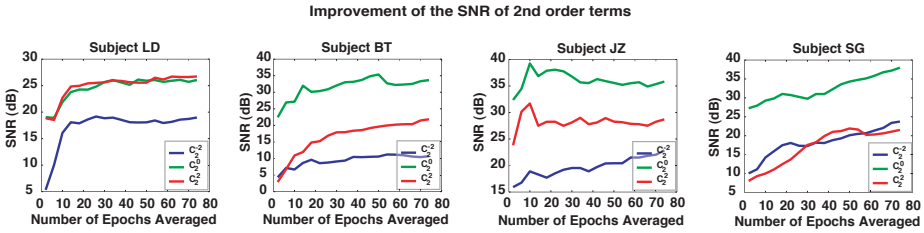

Fig. 4. Improvement of the signal to noise ratio (S/N ratio) in the measurements of 2nd order aberrations with running averages. In all graphics the x-axis is the number of epochs averaged, while the y-axis is the S/N ratio in decibels. Defocus appears in green, and astigmatism in red and blue. It is worth noticing that power dB are a logarithmic scale, not a linear one.

sensor) ranging, for the red stimulus, from approximately 0.43 m for LD to 0.92 m for SG, corresponding to a focusing variability of 0.72D (for the 4.5mm diameter pupil used for the analysis). However, the accommodative change between the red and blue stimuli was around 0.1 m (0.14D) for all subjects.

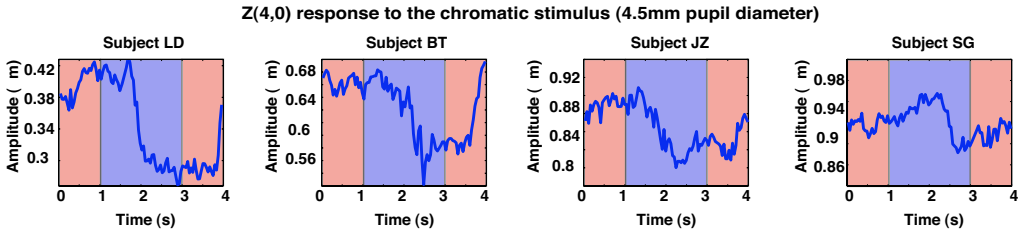

Fig. 5. Average response of accommodation to the red-blue stimulus described in section 2.2 for the four participating subjects. In all cases an average of 75 epochs is shown. As before, the background colour represents the corresponding colour of the stimulus at that time.

3.2. Signal improvement of higher order aberrations

A very important benefit of this methodology is the possibility of studying very small changes in the higher order modes that would typically be buried under the signal noise. In Fig. 6 we present an example of the improvement in the S/N ratio of higher order modes. Mode C_5^{-1} for subject LD is shown. This is a higher order comma like aberration. These results indicate that it varies with accommodation, which supports the hypothesis that at least some of it is produced by the crystalline lens. Fig. 6(a) shows in black one single epoch without averaging, and in red the average of 10 epochs. Fig. 6(b) shows in black the average of 30 epochs and in red 70 epochs. Note the change in scale of the y-axis. The background colours represent again the corresponding colour of the stimulus at that point in time.

In contrast with defocus where the S/N ratio is high and the signal trend is visible even for one single epoch, in the case of higher order aberrations, the S/N ratio can be very low and the signal only be visible after averaging. In Fig. 7 we show the improvement in S/N ratio as a function of epochs averaged. The top panels show the change in S/N for 3rd order aberrations and the bottom panels show this for 5th order aberrations. Each column shows a different subject.

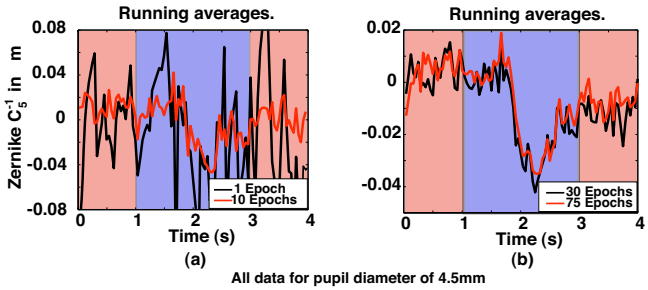

Fig. 6. Impact of running averages in the measurement of higher order aberrations. (a) Single measurement of C_5^{-1} in black, average of 10 epochs in red. (b) Average measurement of C_5^{-1}; 30 epochs in black and 75 in red.

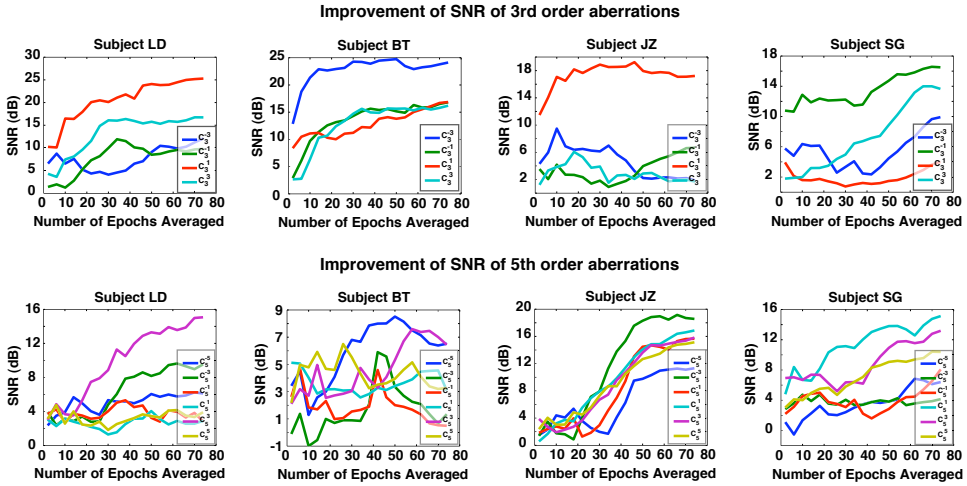

Fig. 7. Improvement of signal to noise ratio (S/N ratio) of higher order aberrations with running averages. In all figures the x-axis is the number of epochs averaged, while the y-axis is the S/N ratio in decibels. The top row shows 3rd order aberrations, and the bottom row shows 5th order aberrations. It is worth noticing that power dB are a logarithmic scale, not a linear one.

3.3. Correlation of Zernike terms with defocus

Figure 8 shows the effect of running averages when investigating correlation between Zernike terms. Panels (a) and (b) show the value of defocus (C_2^0) in the x-axis, against oblique astigmatism (C_2^{-2}) in the y-axis. Panel (a) shows the scatter plot for one single epoch in blue and for an average of 10 epochs in red. The correlation coefficient between these two Zernike modes increases from -0.39 without averaging to -0.51 with 10 epochs. Further averaging, in panel (b), leaves the correlation coefficient almost unchanged. Panels (c) and (d) show defocus (C_2^0) in the x-axis against vertical secondary coma (C_5^{-1}) in the y axis. The correlation coefficient goes in this case from 0.25 for no averaging to 0.6 with 10 epochs, to 0.74 for 75 epochs. So, what seemed a very weak correlation for 1 single epoch, becomes a strong correlation after an average of 75 epochs.

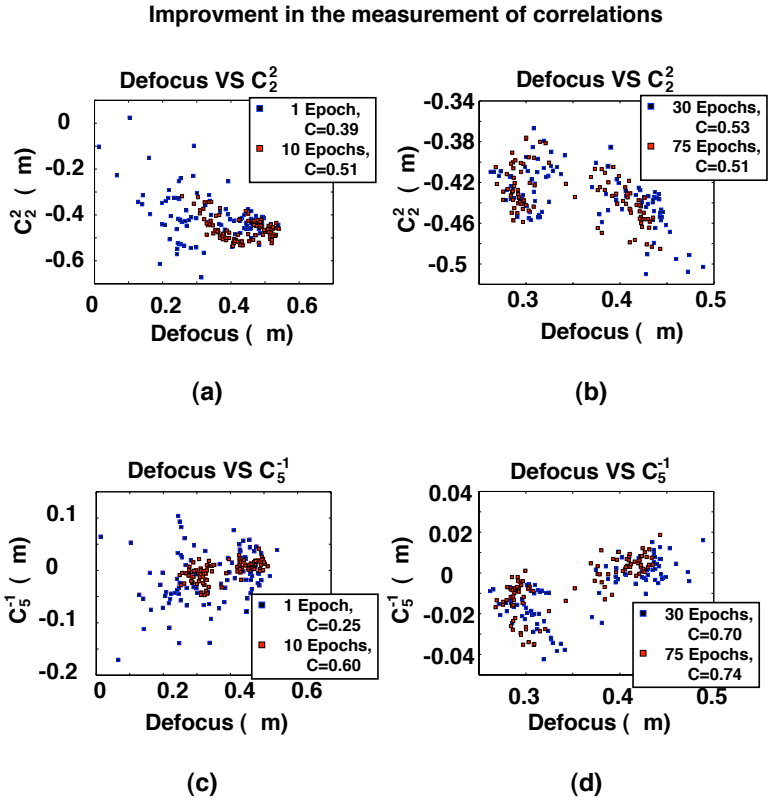

Fig. 8. Example scatter plots showing the correlation between changes in defocus and changes in astigmatism ((a) and (b)) and between changes in defocus and changes in one of the 5th order terms ((c) and (d)) for subject LD. (a) and (c) show in blue the resultant scatter plot for one epoch, and in red for an average of 10 epochs. (b) and (d) show in blue the scatter plot for an average on 30 epochs and in red for 75 epochs. Correlation coefficients are for each case are shown in the insert in each plot

Figure 9 shows the correlation between the changes in each individual Zernike term and the changes in defocus induced by accommodation. The bars have been colour coded, so that the coefficients of each Zernike pair are shown in the same colour. The top row shows the resultant correlation after averaging 75 epochs, whilst the second row shows the result of averaging 10 epochs only. Practically all terms show a better correlation with defocus after a large number of averages. The bottom row shows the colours corresponding to the individual Zernike pairs.

3.4. Amplitude changes and rotation of Zernike terms

Figure 10 shows, for subject LD three examples of how the angle and amplitude of Zernike pairs are linked to accommodation. All cases are for averages of 75 epochs. The first column shows Zernikes $C_3^{\pm 1}$, the second column shows terms $C_5^{\pm 5}$ and the right column shows terms $C_4^{\pm 4}$ In all cases the blue line is the temporal behaviour of the defocus term. In the top panels the red plot shows the changes in amplitude of the Zernike pair when combined with Eq. 1. The

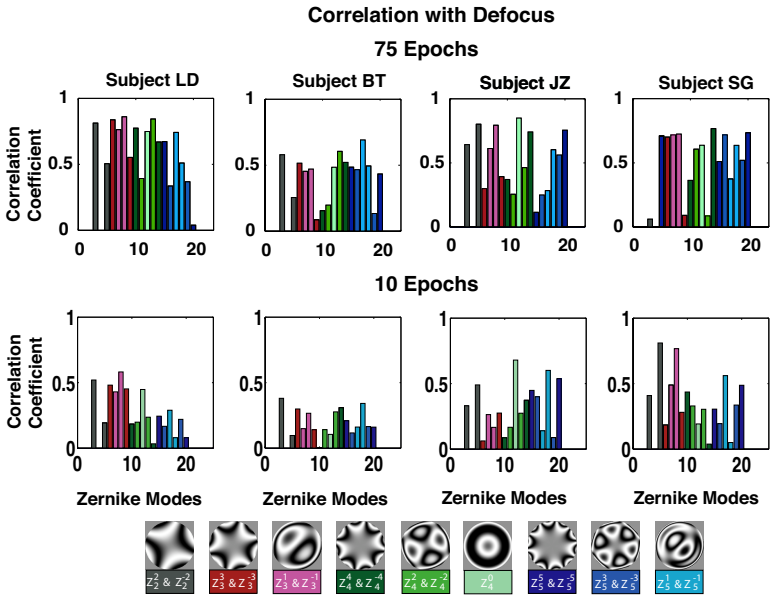

Fig. 9. Absolute value of the correlation coefficients between defocus and each individual Zernike term for all subjects (95% confidence). The top row shows the correlation values for an average of 75 epochs while the second row shows them for an average of 10 epochs. Zernike pairs that can be coupled using Eqs. 1 and 2 are shaded in the same colour. The key is show in the bottom row.

bottom panels show in red the changes in angle of the Zernike pair when coupled with Eq. 2.

Figure 11 shows the correlation between Zernike pairs and defocus. Each Zernike pair has been converted into its angle and amplitude using Eqs. 1 and 2, and these values correlated with the defocus term. The blue bars show the absolute value of the correlation coefficient between defocus and amplitude of the Zernike pair, whilst in red it is show the correlation of defocus with the angle of the Zernike pair. Each Zernike pair has been labelled with capital letters A to I. The key also shows the same colour code used in Fig. 9.

4. Discussion

We have designed and implemented a wavefront sensor and developed a methodology that permits to measure very small changes in aberrations and correlate them with accommodation. The standard deviation of the wavefront RMS over time for higher order aberrations was typically 0.04 m. Running averages allowed detecting changes in higher order aberrations from 0.006 m to 0.02 m and correlate them with amplitude changes of accommodation as small as 0.14D. In a similar fashion as is routinely done in electrophysiology, we can now pick-up ocular higher order aberration signals that would otherwise be below the noise level of an individual measurement.

The design of the instrument permits an easy change of the stimulus presented to the subject without having to modify the instrument itself. By using the hot mirror we can better simulate normal conditions of accommodation than those typically obtained in monocular or/and narrow field instruments. We expect in the future to be able to perform further studies of aberration dynamics during several different visual tasks, such as reading, or some standard psychophysical tests.

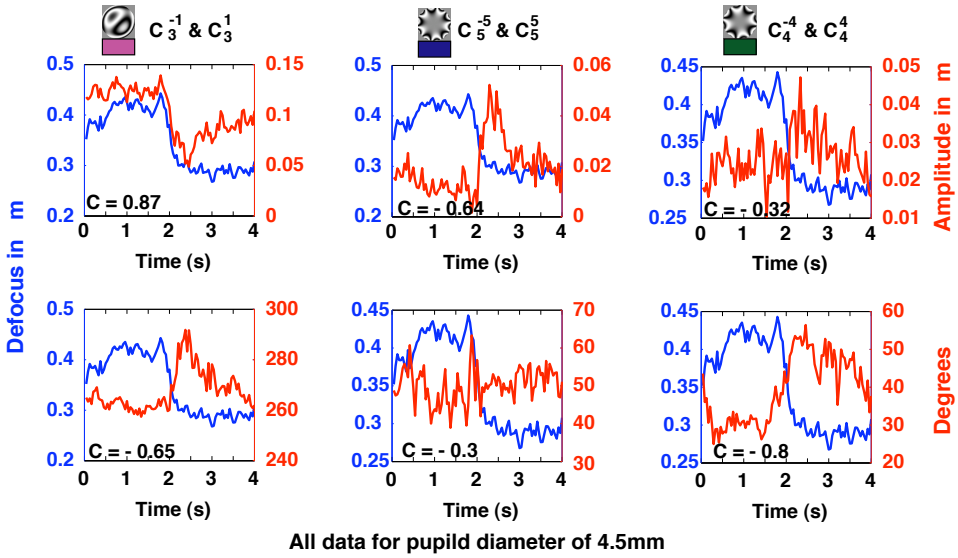

Fig. 10. Examples of how changes in defocus correlate with changes in amplitude and/or angle of other Zernike terms. All plots show in blue and in the left y-axis changes in defocus. In red and in the right y-axis are shown changes in amplitude (top row) or angle (bottom row) of $C_3^{\pm 3}$ (first column), of $C_5^{\pm 5}$ (second column) and of $C_4^{\pm 4}$ (third column)

4.1. Accommodation and higher order aberrations response

The strategy used to analyse the data can be used not only with wavefront sensors but also with autorefractors like the Shin-Nippon SRW-5000 that allows continuous recording at up to 60Hz and with very high precision [20]. The methodology proposed here permits analysis of the systematic changes in accommodation with time produced by a periodic stimulus and eliminates from the signal all the random fluctuations in the measurement introduced by both the eye, and the system used.

Typical wavefront aberration measurements in the human eye have low S/N ratios for most of the higher order aberrations. Consistent with past studies we found second order, third order and spherical aberrations to have higher S/N ratio than all other Zernike terms. These other terms tend to be very small and changes in their amplitudes only evident for larger accommodation changes than those reported in this paper.

Our methodology showed an important improvement in S/N ratio for most higher order aberrations. We have shown that in the absence of a significant number of averages, correlation between accommodation and higher order aberrations stays low. Fig. 9 shows that almost all Zernike terms show a moderate (0.5) to high (0.8) correlation coefficient with defocus when running averages are used, even for those subjects and Zernike terms where the improvement in S/N ratio was lowest.

Correlation between accommodation and practically all Zernike terms should not be a surprise. During accommodation the shape of the crystalline lens changes, effectively producing a different wavefront, and a different polynomial interpolation. As the changes in shape of the crystalline lens must be related to accommodation so must be the change in aberration.

In this context we have also explored the alternative representation of pairing Zernike terms and use an angle and amplitude representing the pair, as is traditionally done for astigmatism in optometric practice. This representation has the advantage that rotations of the optical element

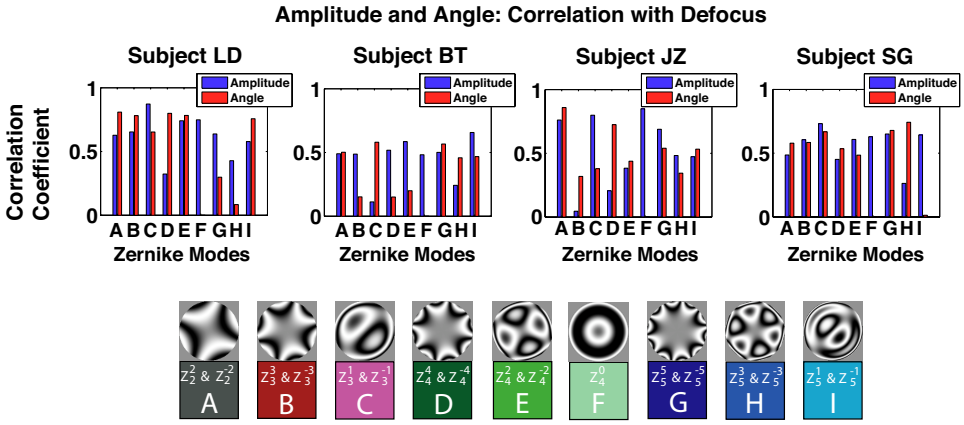

Fig. 11. Absolute value of the correlation coefficients between defocus and the individual Zernike terms expressed as amplitude (blue) and angle (red). Each zernike pair is coded as letters A to I. The key at the bottom of the figure uses the same colours as Fig. 9

are evident as a change in angle but not in amplitude. We see from Eq. 1 that if we vary one of the coefficients, say C_n^m and keep the amplitude of a_{nm} constant, then Eq. 1 defines a circle of radius a_{nm}. Hence, if $C_n^{\pm m}$ changes satisfying this condition, θ_{nm} is forced to rotate. Consequently, what seems to be a change in both coefficients C_n^m and C_n^{-m} can in some cases be the result of a rotation of the optical element without a change in amplitude. In the case of the eye this could be a rotation of the eyeball or one of its optical elements. We also see that a change in amplitude a_{mn} will be followed by a change of angle, unless the ratio between C_n^m and C_n^{-m} stays constant. In this latter case the amplitude can only take values equal to

$$a_{nm} = C_n^m \sqrt{A^2 + 1} \tag{3}$$

where $A = C_n^{-m}/C_n^m$ is constant.

This representation may be of particular value when splitting the effects of torsion from those of accommodation, which as far as the authors are aware has not been yet done. Given the versatility of our system, a second CCD camera could be used to monitor torsion and head rotations. Rotations could then be easily subtracted from the data in this representation yielding the actual change in amplitude of the aberrations.

The results shown in Fig. 10 are of special interest. The first column shows a change in both angle and amplitude. This would be expected if both members of the Zernike pair change independently of each other. The middle column, shows a case in which only amplitude is correlated with defocus, but not the angle. However if we look carefully at the plot for the angle we see that the first half of the signal has some periodic oscillations of about 10 degrees in size. At the point where defocus changes they disappear turning into a smoother signal. Although we do not observe a *linear* correlation with accommodation we see a change in the behaviour of the signal paired with accommodation. The origin of these oscillations is not clear. They could be an artefact of a very low signal value in C_n^{-m} in Eq. 2, introducing exaggerated values of θ when the noise dominates and the signal is averaged to a value close to zero. The last column shows a strong correlation between angle and accommodation but a very small one with the amplitude of the Zernike pair. Again in this case we observe a different behaviour in this signal before and after the change in accommodation. The presence of these non-linear correlations in some terms deserve further studies, to clarify if they are the result of a very noisy signal or

they are in fact of that form.

An important topic we have not addressed is if changes in higher order aberrations show any trends across subjects. In order to address this issue a much larger sample is needed. The aim of this study was to develop the system and validate the methodology to look at these trends in a larger population in the future.

4.2. Limitations of the technique

It is important to understand the limitations of this technique. The technique has enabled much more precise measurments to be made so the nature of aberrations, and their time course and their relation to accomodative changes can be described in much more detail. However, this methodology is not suited to study other random processes that may occur during accommodation. All the fluctuations varying randomly in time in the accommodative process are removed by the method of analysis. Moreover, all of the changes in aberrations occurring at frequencies different to that of the stimulus or its harmonics will be averaged out with this method. For example, changes in aberrations induced by the cardio-pulmonary system will not appear in our method of analysis, and their impact in accommodation cannot be studied with this method.

We are able to pick up all of the signal that changes consistently at the frequency of the stimulus or its harmonics. The value of this is shown in Fig. 5 where we observe very similar trends for all four subjects, which would have been impossible otherwise, as these trends would have been masked out by random fluctuations in accommodation.

5. Conclusion

In this paper we have presented a methodology to measure the systematic changes of aberrations induced by changes in accommodation with small amplitudes. By averaging epochs, we have measured changes in higher order aberrations from 0.006 m to 0.02 m and correlated them with amplitude changes of accommodation as small as 0.14D. These small changes would have been undetectable without epoch averaging. The correlation coefficients of Zernike terms with defocus were calculated, demonstrating higher values of correlation for epoch averaging. The accurate monitoring of defocus at the start of the accommodation response has shown some interesting trends that may be related with the mechanisms behind accommodation. The improvement this methodology brings about in measuring low amplitude aberrations that are driven by accommodation, or any other periodic process, opens up new paths in understanding the process of accommodation and the mechanisms behind aberration dynamics.

There is a vast literature in electrophysiology that uses the running average technique to extract signals from noisy backgrounds and a very good review of them can be found in Regan's book on Electrophysiology [21]. Different methods and approaches have been used over the years. The vision community is familiar with this literature and could very well make use of these methods in order to better understand aberration dynamics.

Acknowledgments

We are indebted to Prof. Henrik Jenssen from Imperial College for very useful discussions during the undertaken of this work. This project has been funded by EPSRC Grant GR/S58812/01(P) and by the National University of Ireland, Galway, sub-contracted to SHARP-EYE FP6 Research Training Network, Contract EC FP-5 HPRN-CT-2002-00301. Vincent Guériaux is an undergraduate student at Université Paris-Sud 11, IFIPS – Optronics department. His participation in this project was part of a engineering-trainee internship at City University.